Unraveling mechanisms of vascular remodeling in arteriovenous fistulas for hemodialysis

Wong, C.Y.

Cover Page

Universiteit Leiden

Leiden University
Repository

The handle http://hdl.handle.net/1887/46406 holds various files of this Leiden University dissertation.

Author: Wong, C.Y.
Title: Unraveling mechanisms of vascular remodeling in arteriovenous fistulas for hemodialysis
Issue Date: 2017-03-08

Chapter 4

A novel murine model of arteriovenous fistula failure:
The surgical procedure in detail

Wong, C.Y., de Vries, M.R., Wang, Y., van der Vorst, J.R., Vahrmeijer, A.L., van Zonneveld, A.J,
Hamming, J.F., Roy-Chaudhury, P., Rabelink, T.J. , Quax, P.H.A. and Rotmans, J.I.

Abstract

The arteriovenous fistula (AVF) still suffers from a high number of failures caused by insufficient remodeling and intimal hyperplasia from which the exact pathophysiology remains unknown. In order to unravel the pathophysiology a murine model of AVF-failure was developed in which the configuration of the anastomosis resembles the preferred situation in the clinical setting. A model was described in which an AVF is created by connecting the venous end of the branch of the external jugular vein to the side of the common carotid artery using interrupted sutures. At a histological level, we observed progressive stenotic intimal lesions in the venous outflow tract that is also seen in failed human AVFs. Although this procedure can be technically challenging due to the small dimensions of the animal, we were able to achieve a surgical success rate of 97% after sufficient training. The key advantage of a murine model is the availability of transgenic animals. In view of the different proposed mechanisms that are responsible for AVF failure, disabling genes that might play a role in vascular remodeling can help us to unravel the complex pathophysiology of AVF failure.

Introduction

A functional vascular access conduit is of vital importance for patients with renal failure that depend on chronic hemodialysis to stay alive. The construction of an arteriovenous fistula (AVF) is currently the preferred choice for vascular access. However, AVF related complications constitute a major cause of morbidity for patients on chronic hemodialysis. Despite extensive scientific efforts, none of the novel approaches to reduce AVF access-related complications did result in substantial improvement of AVF durability. Part of this disappointing progress relates to incomplete understanding of the underlying pathophysiology of hemodialysis access failure. To unravel the pathophysiology of AV access failure, animal models that closely mimic human pathology are of utmost importance. In this respect, not only the animal species but also the anastomotic site, the required anti-coagulatory therapy and the duration of follow up after surgery should be taken into account[1]. While large animals are the most suitable for intervention studies aimed to develop new therapeutic strategies, murine models have the greatest potential to gain more insight in the molecular mechanisms underlying AV access failure due to the availability of transgenic mice. In addition, a large number of mice can be used for this purpose at lower costs compared to larger animal use.

The first murine model of AVF failure was described in 2004 by Kwei and coworkers[2]. In this model, AVFs were constructed using the carotid artery and the jugular vein in an end-to-end manner using an intravascular catheter. This model could be useful to study early venous adaptation in AVFs although the end-to-end configuration and the presence of an intravascular catheter limit the validity of this model for human AVFs. An improved AVF model was introduced by Castier and coworkers3 in which the end of the carotid artery is connected to the side of the jugular vein. However, AVFs in hemodialysis patients are usually constructed by anatomizing the end of a vein to the side of an artery. The exact configuration of the AVF is a crucial characteristic of an AV access model since it determines the hemodynamic profile within the conduit4. The latter is an important contributor to endothelial dysfunction and subsequent development of intimal hyperplasia (IH) [5].

A novel murine model was recently developed with an identical anatomical configuration as is utilized in humans[6]. In this model, AVF are created in C57BL/6 mice by anastomosing the end of a branch of the external jugular vein to the side of the common carotid artery with interrupted sutures. In the present paper, we focus on the microsurgical procedure of this model in order to facilitate the widespread use of this murine model, aimed to unravel the complex pathophysiology of hemodialysis access failure.
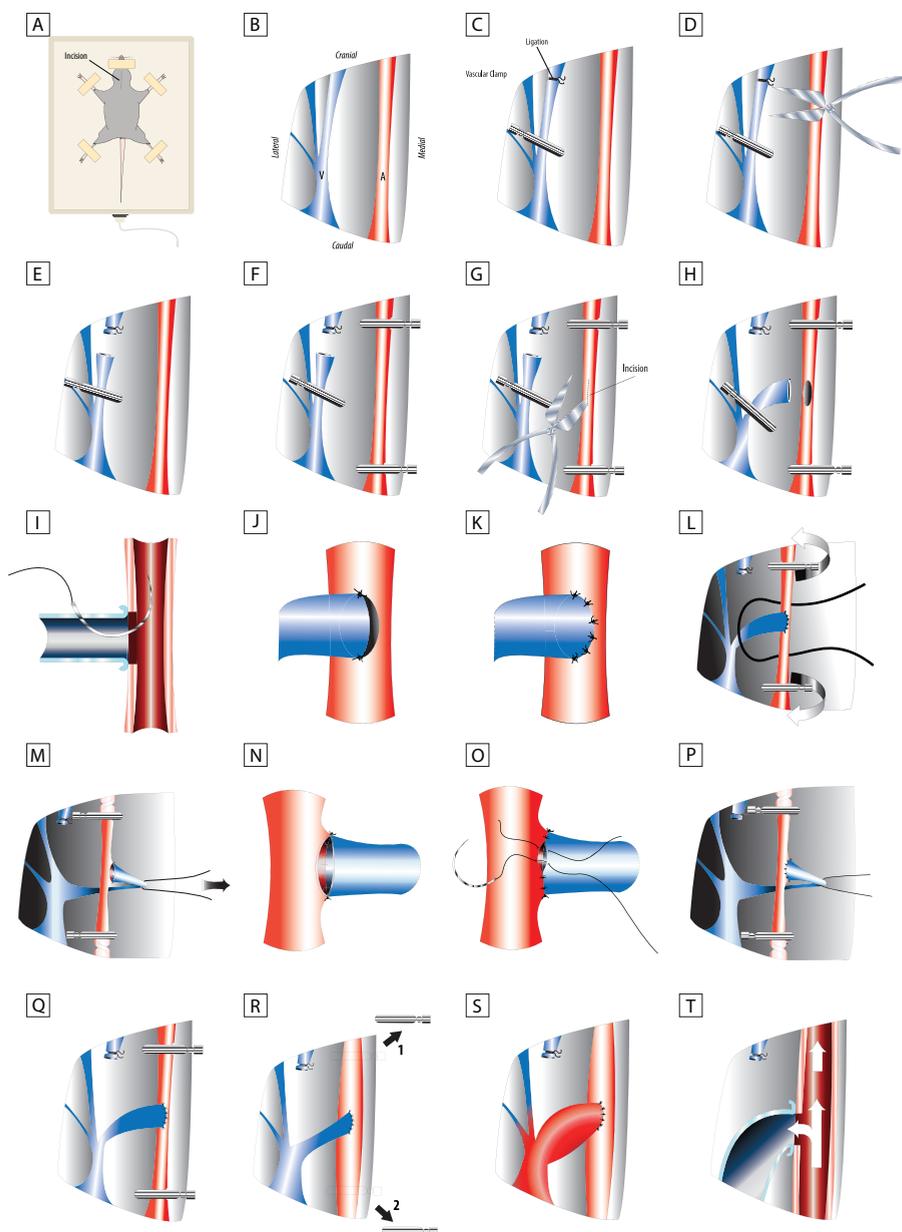
Figure 1. Detailed scheme of surgical procedure. (A-T) Key steps for successful creation of an AVF.

Protocol:

All experiments were approved by the committee on animal welfare of the Leiden University Medical Center.

1. Animal preparation and anesthesia

1.1 Anesthetize the mouse (1-3 months old) in a continuous anaesthetic induction chamber filled with 3-4 % isoflurane.

1.2 Shave the ventral side of the neck and the inside part of the left upper leg using an electrical razor and use a piece of tape to remove the hair.

1.3 Apply ocular ointment on both eyes.

1.4 Position the animal on the heating blanket on which the nose ventilation mask is fixed. Fixate the head to the nose mask using adhesive tape. Deliver isoflurane at a concentration of 1.5-2.0 % using oxygen enriched air set at the following flow: air 0.3 L/min, 100% oxygen 0.2 L/min. Pinch the skin between the toes to assess the depth of anaesthesia and adjust the concentration of isoflurane if needed.

1.5 Fixate the animal to the heating blanket with adhesive tape on all the limbs that is set at approximately 37 °C in a supine position.

1.6 Inject buprenorphine dissolved in sodium chloride (NaCl) 0.9% at a dosage of 0.1 mg/kg together with 0.5 mL of sterile NaCl 0.9% subcutaneously in the flank of the animal.

1.7 Apply chlorhexidine tincture 0.5% to the prepared area.

2. Skin incision

2.1 Position the animal under the microscope with its head towards the surgeon.

2.2 Make a longitudinal incision of approximately 1.5 cm in the midline of the ventral neck using a micro scissor.

2.3 Grab the salivary glands with forceps and displace the right salivary gland cranially until it is partly outside the wound.

3. Dissecting and preparing the vein

3.1 Identify and bluntly dissect the dorsomedial branch of the right external jugular vein completely from its perivascular tissue by spreading just alongside and in the direction of the blood vessel.

3.2 Place a loop (10.0 suture) around the dissected vein and apply one knot without locking it.

4. Removing the sternocleidomastoid muscle

4.1   Using forceps, bluntly dissect the right sternocleidomastoid muscle from its surroundings by spreading along its border. Place a pair of open forceps under the isolated muscle and ligate it proximally and distally with a 6.0 suture. Subsequently, excise the muscle using a cauterizer.

5. Dissecting and preparing the common carotid artery

5.1   Identify and dissect the right common carotid artery using forceps. Place a 6.0 suture thread around the artery to aid in the manipulation of the artery.

5.2   Apply vascular clamps as distally and proximally as possible.

5.3   Make a longitudinal incision in the middle of the artery of approximately 1 mm using the specialised micro scissor.

5.4   Rinse the artery with a heparin solution [100 IU/mL] until the vessel is clear of blood.

5.5   Measure and adjust the length of the incision if necessary to match the width the vascular clamp [1.1 mm].

6. Ligation of the vein

6.1   Apply a vascular clamp proximally of the already prepared vein and place a suture thread around the vein.

6.2   Apply gentle caudal traction to the vein using a haemostat that is placed on the suture thread and ligate the vein as distally as possible using the 10.0 suture that was placed earlier.

6.3   Cut the vein using a scissor just proximally to the ligation.

6.4   Using vascular forceps, gently open the lumen of the vein and rinse it with a heparin solution [100 IU/mL].

7. Creation of anastomosis part 1

7.1   Connect the vein to the artery with an interrupted suture (10.0) using 2 square knots at the twelve o'clock position followed by a suture at the six o'clock position. Make sure to connect the vein to the artery without allowing it to rotate around its own axis. Rotate the animal in order to improve the surgical exposure.

7.2   Position a suture thread around the vein and apply gentle lateral traction using a haemostat.

7.3   Using the same interrupted sutures, complete the anastomosis by placing approximately 3-4 additional sutures at the visible ventral side of the anastomosis.

8. Heparin administration

8.1   Rotate heating blanket 180 degrees and focus the microscope on the left upper leg.

8.2   Identify the femoral vein/artery/nerve bundle by looking for a vascular structure that runs longitudinally in the medial part of the upper leg and can be seen through the skin. Make an incision with the micro scissor of approximately 1 cm directly above the femoral vein in a lengthwise manner.

8.3   Carefully dissect the perivascular tissue of femoral vein and inject heparin at a dose of 0.2 IU/gram bodyweight in the femoral vein.

9. Creation of anastomosis part 2

9.1   Return to the neck area and remove the suture thread that was placed around the vein.

9.2   Place a suture thread (6.0) that subsequently passes below the carotid artery, over the vein and again below the carotid artery. (Figure 1-L)

9.3   Remove the venous vascular clamp.

9.4   Next, twist the half completed arteriovenous fistula 180 degrees along the axis of the carotid artery in a clockwise manner by simultaneously twisting both the vascular clamps and apply medial traction to the ends of the suture thread.

9.5   Complete the anastomosis in the same fashion as is described in step 7.2.

10. Vascular clamp removal

10.1   Remove the suture thread and rotate the vascular clamps 180 degrees counter clockwise.

10.2   Remove the distal vascular clamp followed by the proximal vascular clamp.

10.3   Assess the patency of the anastomosis by gently occluding the venous outflow tract with the vascular forceps. In case of a patent anastomosis, the pre-occluding venous section will expand in a pulsatile fashion. Relocate the right salivary gland to its original anatomical position using forceps.

11. Skin closure and postoperative care

11.1   Close the skin of the upper leg with an uninterrupted suture (6.0).

11.2   Close the skin of the neck with an uninterrupted suture (6.0).

11.3   Remove the animal from the heating blanket and inject 0.5 mL NaCl 0.9% subcutaneously.

11.4   Place the animal in a darkened cage that is heated with a heating lamp and let it recover fully. When an animal does not recover fully, make sure it does not suffer from a hemodynamic shock due to bleeding in the surgical area. Look for signs such as a swollen neck and the leakage of blood.

11.5   After approximately 6 hours after the first injection of buprenorphine, inject a single dose of a sustained-release formulation of buprenorphine subcutaneously in a dose that is recommended by the manufacturer, in order to provide adequate analgesia for an additional 72 hours.

12. Tissue harvesting

12.1   Anesthetize the animal with an anesthetic-mixture containing midazolam (5 mg/kg), medetomidine (0.5 mg/kg) and fentanyl (0.05 mg/kg) administered intraperitoneally.

12.2   Fixate the animal in a supine position by inserting needles through its paws and cheeks into a non-heated silicon mat.

12.3   Make an incision of approximately 1.5-2.0 cm over the scar in the neck with the micro scissor.

12.4   Dissect the AVF, and place suture threads (6.0) around the proximal-, distal artery and venous outflow tract for easy identification.

12.5   Assess the patency of the AVF as is described in section 10.3 of the protocol.

12.6   Open the peritoneal cavity by performing a medial laparotomy using the micro scissor.

12.6.1   Cut through the left and right ventral rib cage using a pair of scissors starting caudally in the midclavicular line. Using a micro scissor, transect the diaphragm that is attached to the middle part of the ventral rib cage and subsequently displace this section cranially using forceps.

12.6.2   Locate the inferior caval vein and transect it with a micro scissor.

12.7   Insert a needle 23 gauge needle in the left ventricle and perfuse with PBS at a pressure of approximately 100 mmHg until the intravasal fluid is nearly clear.

12.8   Without removing the needle, now perfuse with 4% formalin for 10 minutes at a pressure of approximately 100 mmHg.

12.9   Excise the AVF by transecting both the arteries and vein with the micro scissor and submerge it in a 4% formalin solution overnight.

13. Tissue embedding and sectioning

13.1   Process the tissue to paraffin according to the manufacture's protocol. The protocol applied consisted of the following:

13.1.1   Immerse in Ethanol 70% for 1 hour at room temperature. Repeat 2X.

13.1.2   Immerse in Ethanol 96% for 1 hour at room temperature. Repeat 2X.

13.1.3   Immerse in Ethanol 99.5% for 1 hour at room temperature. Repeat once.

13.1.4   Immerse in Ethanol 99.5% for 1.5 hour at room temperature.

13.1.5   Immerse in xylene 100% for 1 hour at room temperature. Repeat once.

13.1.6   Immerse in Paraffin for 1 hour at 62°C. Repeat 2X.

13.2 Embed the AVF in paraffin so that the venous outflow tract is orientated perpendicular to the embedding cassette.

13.3 Using a microtome, create 12 serial sections each consisting of 30 sections with a 5 μm thickness. Then of each serial section, place one section on a single mounting glass starting from position one up to twelve in an orderly fashion starting with the area closest to the anastomosis.

Representative results

After the creation of the anastomosis (Figure 1), the patency should be assessed by shortly occluding the venous outflow tract with a vascular forceps. When the anastomosis is patent, the vascular tract proximal to the occlusion should clearly expand in a pulsatile manner. In addition, the patency is confirmed by using near infrared fluoroscopy (NIRF) that effectively functions as an angiography (Figure 2). A failure in the surgical procedure can lead to an occlusion of the anastomosis as is depicted in (Figure 2). This failure can be caused by a too narrow anastomotic area, torsion of the vessels, inadequate heparin dose or an accidental suture placement that connects the front side of the anastomosis to the back side.

At a histological level, the process of vascular remodeling in AVF can be investigated elegantly using this model. Vascular remodeling in AVF occurs as a result of the increase in blood flow and pressure. In mice, this response is characterized by an increase in circumference (e.g. outward remodeling) leading to an increase in luminal area in the first 2 weeks after surgery. After these 2 weeks, the luminal area progressively decreases due to a stop in the outward remodeling and ongoing thickening of the tunica intima. The formation of these progressive stenotic lesions results in occlusion of 50% of AVF at 4 weeks after surgery. Therefore, the optimal time point to harvest the AVFs would be at 2 weeks after surgery, since in this phase, proper analysis of the vascular response in patent AVF is still feasible. Immunostaining of the venous outflow tract at 2 weeks after surgery shows that the cellular compartment of the intima mainly consists of alpha-smooth muscle actin (α-SMA) positive cells (Figure 3), as observed in failed human AVFs as well[7.]

In view of the complexity of the microsurgical procedure, it's realistic to reckon with technical failure of the procedure in a proportion of the mice. In our hands, the success rate of the procedure was 67% in the beginning. However, with further training this rate was increased up to 97%. The main cause of failure was hemorrhage (60%), followed by acute thrombosis (27%) and anesthesia- related death (13%). After sufficient training, the surgical procedure can be performed in approximately 1 hour.
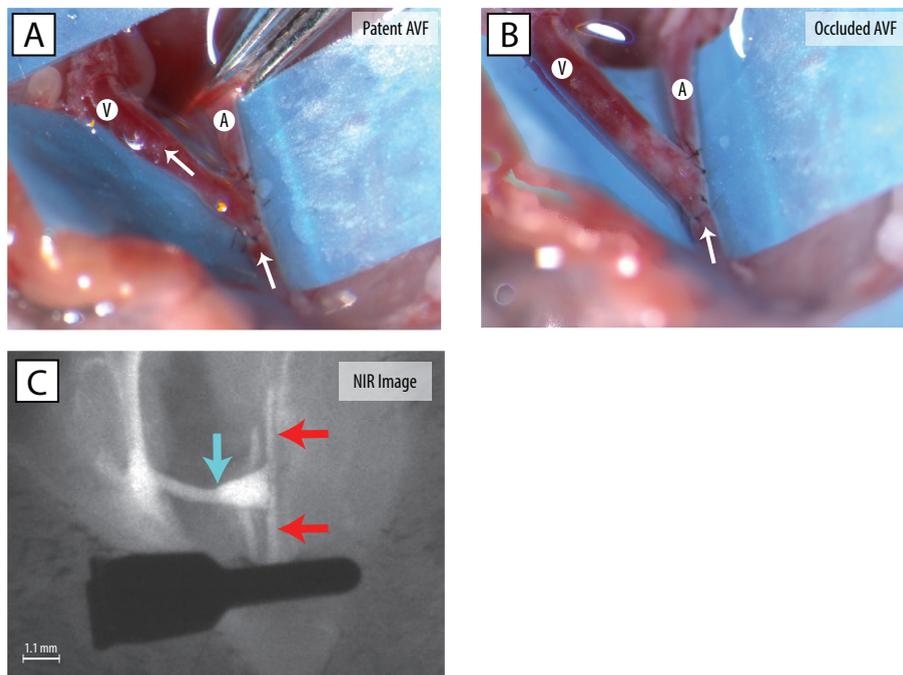
Figure 2. Macroscopic pictures of patent and occluded AVFs. (A) A patent AVF with a vascular clamp on the distal common carotid artery. (B) An occluded AVF. (*White arrow*) indicates the direction of the blood flow. (C) A patent AVF demonstrated using Near Infrared Fluoroscopy. (*red arrow*) indicates artery. (*blue arrow*) indicates venous outflow tract.
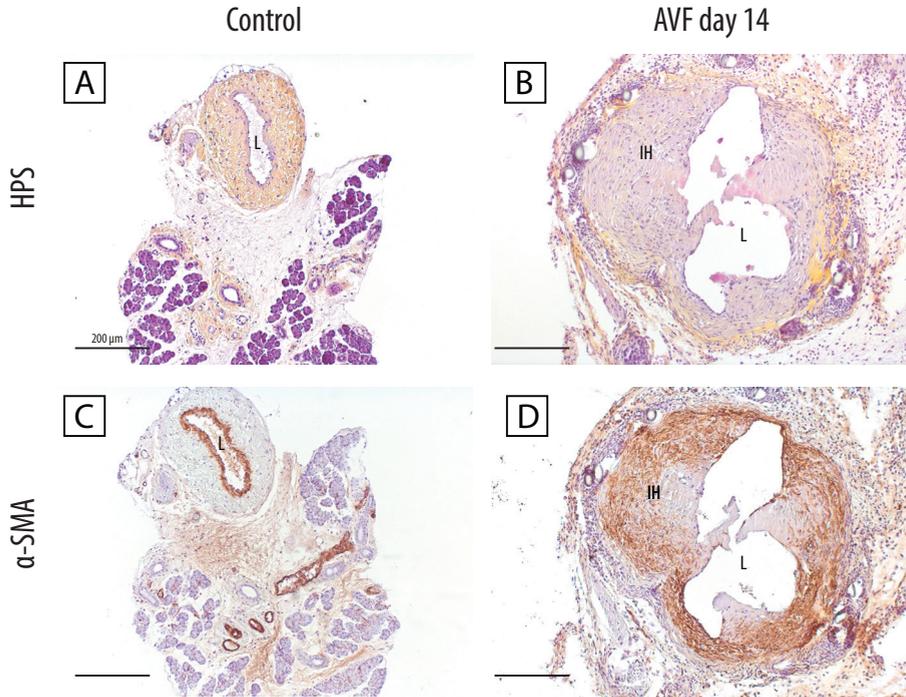
Control

AVF day 14

Figure 3. Histological stainings of the venous outflow tract of the AVF at day 14 versus unoperated control vessels. (A-B) Morphologic overview using hematoxylin, phloxin and saffron showing a clear increase in vessel circumference and intimal hyperplasia development 14 days after AVF creation. (C-D) Immunohistochemical staining demonstrating that the majority of the cells present the intimal hyperplasia are alpha smooth muscle actin positive. *(L) Lumen*; *(IH) Intimal hyperplasia; scale bar: 200 μm*

Discussion

The AVF is considered to be the Achilles' heel in hemodialysis treatment. Unfortunately, the AVF still suffers from a high number of failure[8-10]. Despite extensive research on the underlying mechanisms, the exact pathophysiology remains unknown. Numerous murine models for AVF failure have already been described in literature [2,3,11,12]. However, none of these models incorporate a venous end to arterial side anastomosis configuration that is most used in the clinical situation. This is very relevant since the resultant hemodynamic profile plays an important role in vascular remodeling. Moreover, some of the models used a synthetic cuff for the connection between the artery and vein [2,11], which is not used in the clinical setting.

To improve the clinical relevance, we therefore developed a murine model in which a unilateral venous end to arterial side anastomosis was created between a branch of the jugular vein and common carotid artery with interrupted sutures6. In this model crucial histomorphological changes were observed including outward remodeling and progressive intimal hyperplasia, ultimately leading to AVF failure.

A crucial aspect of the surgical procedure is the anaesthesia protocol. It is recommended to use isoflurane inhalation anaesthesia, as this is a safe and easy method for obtaining prolonged periods of anaesthesia. The latter is especially important for the training phase in which the whole procedure can take up to 3 hours.

In order to create the necessary room for the traversing outflow vein of the arteriovenous fistula, the ipsilateral sternocleidomastoid muscle needs to be excised.

With respect to the vessel handling during surgery, dissection of vessels should be performed in a blunt manner using forceps. The use of specialised vascular straight forceps are recommended for direct handling and manipulation of the vessels as they provide more precision and produce less mechanical damage due to the rounded tip. The usage of suture threads as vessel loops combined with a hemostat can aid in safe tissue handling and moreover, in presenting the tissue in an optimal manner when used as a third hand which is crucial so this procedure can be performed without any direct assistance.

Undoubtedly, the most difficult step in the procedure are the suture placements between the artery and vein. Care must be taken not to suture the "back"-side of the anastomosis with the "front"-side, as this will lead to narrowing of the anastomosis that can lead to early failure of the AVF. To prevent this from happening, position the tip of the vascular forceps between the two walls of the vessel in order to separate them. The technical difficulty can be considered to be a limitation of this model. However, we do not think that this procedure is more challenging than the model that is presently most widely used[3,6].

It's difficult to make a general remark on the sample size for future studies, as the calculated sample size does not only depend on the variability between animals but also on the 'strength' of the intervention. We estimate that a group size of approximately 10 mice (excluding mice that drop out of the study because of technical failure of the AVF) should be sufficient for studies that focus on the role of a specific gene in AVF failure. Recently, we were able to obtain significant results with an average group size of 10 animals in a study on the role of elastin in murine AVF remodeling[13].

One aspect of our murine model requires further discussion. It is known that the uremic milieu in patients with end stage renal disease contributes to a multitude of vascular diseases including venous intimal hyperplasia even prior to hemodialysis access surgery[14-16]. This present model does not incorporate the uremic milieu. Therefore, the incorporation of a model of chronic

renal failure [17] would be a valuable additive step to further improve the validity of this murine model.

Acknowledgements

Reference List

1. Rotmans, J.I. Animal Models for Studying Pathophysiology of Hemodialysis Access. *The Open Urology & Nephrology Journal.* **7** 14-21, doi:10.2174/1874303X01407010014 (2014).

2. Kwei, S. *et al.* Early adaptive responses of the vascular wall during venous arterialization in mice. *Am.J.Pathol.* **164** (1), 81-89, doi:S0002-9440(10)63099-4 [pii];10.1016/S0002-9440(10)63099-4 [doi] (2004).

3. Castier, Y. *et al.* Characterization of neointima lesions associated with arteriovenous fistulas in a mouse model. *Kidney Int.* **70** (2), 315-320, doi:5001569 [pii];10.1038/sj.ki.5001569 [doi] (2006).

4. Krishnamoorthy, M.K. *et al.* Hemodynamic wall shear stress profiles influence the magnitude and pattern of stenosis in a pig AV fistula. *Kidney Int.* **74** (11), 1410-1419, doi:ki2008379 [pii];10.1038/ki.2008.379 [doi] (2008).

5. Ene-Iordache, B., Cattaneo, L., Dubini, G., & Remuzzi, A. Effect of anastomosis angle on the localization of disturbed flow in 'side-to-end' fistulae for haemodialysis access. *Nephrol. Dial.Transplant.* **28** (4), 997-1005, doi:gfs298 [pii];10.1093/ndt/gfs298 [doi] (2013).

6. Wong, C.Y. *et al.* Vascular remodeling and intimal hyperplasia in a novel murine model of arteriovenous fistula failure. *J.Vasc.Surg.* **59** (1), 192-201, doi:S0741-5214(13)00553-3 [pii];10.1016/j.jvs.2013.02.242 [doi] (2014).

7. Rekhter, M., Nicholls, S., Ferguson, M., & Gordon, D. Cell proliferation in human arteriovenous fistulas used for hemodialysis. *Arterioscler.Thromb.* **13** (4), 609-617, (1993).

8. Falk, A. Maintenance and salvage of arteriovenous fistulas. *J.Vasc.Interv.Radiol.* **17** (5), 807-813, doi:17/5/807 [pii];10.1097/01.RVI.0000217928.43396.35 [doi] (2006).

9. Tordoir, J.H. *et al.* Prospective evaluation of failure modes in autogenous radiocephalic wrist access for haemodialysis. *Nephrol.Dial. Transplant.* **18** (2), 378-383, (2003).

10. Dixon, B.S., Novak, L., & Fangman, J. Hemodialysis vascular access survival: upper-arm native arteriovenous fistula. *Am.J.Kidney Dis.* **39** (1), 92-101, doi:S0272-6386(02)34055-1 [pii];10.1053/ajkd.2002.29886 [doi] (2002).

11. Yang, B., Shergill, U., Fu, A.A., Knudsen, B., & Misra, S. The mouse arteriovenous fistula model. *J.Vasc.Interv.Radiol.* **20** (7), 946-950, doi:S1051-0443(09)00346-7 [pii];10.1016/j.jvir.2009.03.044 [doi] (2009).

12. Kang, L. *et al.* Regional and systemic hemodynamic responses following the creation of a murine arteriovenous fistula. *Am.J.Physiol Renal Physiol.* **301** (4), F845-F851, doi:ajprenal.00311.2011 [pii];10.1152/ajprenal.00311.2011 [doi] (2011).

13. Wong, C.Y. *et al.* Elastin is a key regulator of outward remodeling in arteriovenous fistulas. *Eur.J.Vasc.Endovasc.Surg.* **49** (4), 480-486, doi:S1078-5884(15)00037-4 [pii];10.1016/j.ejvs.2014.12.035 [doi] (2015).

14. Kennedy, R. *et al.* Does renal failure cause an atherosclerotic milieu in patients with end-stage renal disease? *Am.J.Med.* **110** (3), 198-204, doi:S0002-9343(00)00695-1 [pii] (2001).

15. Cheung, A.K. *et al.* Atherosclerotic cardiovascular disease risks in chronic hemodialysis patients. *Kidney Int.* **58** (1), 353-362, doi:kid173 [pii];10.1046/j.1523-1755.2000.00173.x [doi] (2000).

16. Lee, T. *et al.* Severe venous neointimal hyperplasia prior to dialysis access surgery. *Nephrol.Dial.Transplant.* **26** (7), 2264-2270, doi:gfq733 [pii];10.1093/ndt/gfq733 [doi] (2011).

17. Kokubo, T. *et al.* CKD accelerates development of neointimal hyperplasia in arteriovenous fistulas. *J.Am.Soc.Nephrol.* **20** (6), 1236-1245, doi:ASN.2007121312 [pii];10.1681/ASN.2007121312 [doi] (2009).

Supplemental data

Name	Company	Catalog Number
Dissecting microsocpe	Leica	M80
Forceps	Medicon	07.61.25
Vascular forceps	S&T	JFL-3D.2
Vascular forceps	S&T	D-5a.2
Forceps	Roboz	SS/45
Micro scissor 5 mm blade	Fine science tools	15000-08
Micro scissor 2 mm blade	Fine science tools	15000-03
Scissor	Medicon	05.12.21
Clip applier 1	S&T	CAF-4
Vascular clamp 1	S&T	B-1V
Clip applier 2	BBraun	FE572K
Vascular clamp 2	BBraun	FE740K
Hemostatic forceps	BBraun	BH110
10.0 sutures	BBraun	G1117041
6.0 sutures	BBraun	768464
Cauterizer	Fine science tools	18010-00
Needle holder	Medicon	11.82.18
Ocular ointment	Pharmachemie	41821101
Chlorhexidine tincture 0,5%	Leiden University Medical Center	NA
Heparin	Leo Pharma	012866-08
Buprenorphin	RB Pharmaceuticals	283732
Isoflurane	Pharmachemie	45.112.110
Anesthesia mask	Maastricht university	custom made
Midazolam	Actavis	AAAC6877
Dexmedetomidine	Orion	141-267
Fentanyl	Bipharma	15923002
Continuous anaesthetic induction chamber	Vet-tech solutions	AN010R

Table 1. Materials used for the surgical procedure